DARK ENERGY IN THE UNIVERSE

Modern paradigm of the Universe evolution

$$\cdots\to DS \to FRW\,RD \to FRW\,MD \xrightarrow{\;t_0\;} \widetilde{DS} \cdots\to$$

$a(t)$: $e^{\int H dt}$ ($|\dot H| \ll H^2$), $t^{1/2}$, $t^{2/3}$, $e^{\int H dt}$

$H \equiv \frac{\dot a}{a}$

Existense of dark energy - - kinematical statement assuming the "Einsteinian interpretation"

$$R_i^k - \frac{1}{2}\delta_i^k R = -8\pi G\left(T_{i\,(m)}^{k} + \tilde T_{i\,(DE)}^{k}\right) \quad 4D$$

$T^k_{i(DE);k} = 0$

$\frac{\Delta\Phi}{a^2} = 4\pi G\,\delta\rho_m \Leftarrow$ matter seen through its active gravitational mass (effect on motion of stars, galaxies and light)

Remarkably $\tilde T_{i\,(DE)}^{k} \approx \varepsilon_{DE}\,\delta_i^k$

FRW symmetry: $\varepsilon_{DE}(z)$, $p_{DE}(z)$ — 1 function from background evolution

First-order pert. (scalar, growing) - 1 more function of z

$$\frac{G^2\hbar\,\varepsilon_{DE}}{c^7} = 1.25\cdot 10^{-123}\cdot\frac{\Omega_{DE}}{0.7}\left(\frac{H_0}{70}\right)^2$$

$$\rho_{DE} = \varepsilon_{DE}c^{-2} = 6.44\cdot 10^{-30}\ \mathrm{g\,cm^{-3}}\ (\ldots\ldots)$$

Present matter content of the Universe

(in terms of the critical density

$$\rho_{crit} = \frac{3H_0^2}{8\pi G} \simeq 10^{-29}\ g/cm^3, \quad \Omega_i = \frac{\rho_i}{\rho_{crit}}$$
)

1. Baryons (p, n) and leptons (e)	5 %	
2. Photons (γ)	$5 \cdot 10^{-5}$	
3. Neutrinos $(\nu_e, \nu_\mu, \nu_\tau)$	$< 1\%$	
4. Non-relativistic non-baryonic dark matter	$\approx 25\%$	Not known from laboratory experiments
5. Dark energy	$\approx 70\%$	

Two possible forms and interpretations of DE

1. Physical

New non-gravitational field of matter

Its proper place – in the rhs of eqn.

2. Geometrical

Depends on the Riemann tensor of our 4D or additional dimensions

Its proper place – in the lhs of eqn.
Gravity is modified

No absolute border between these 2 cases

Λ – intermediate case

Investigation of dark energy

I. From observations to theory

Reconstruction program (1998)

1) $H(z)$, $\varepsilon_{DE}(z)$
2) $q(z)$, $p_{DE}(z)$, $w_{DE}(z)$
3) $r(z)$, $\dfrac{dw_{DE}(z)}{dz}$

1. Inversion of classical cosmological tests $\mathcal{D}_L(z) \to H(z)$
2. CMB (acoustic peaks spacing, ISW), BAO
3. $\left(\frac{\delta\rho}{\rho}\right)_m (z)$, $\Phi(z)$ from gravitational lensing, correlation of $\frac{\delta\rho}{\rho}$ with CMB

II. From theory to observations

Models (many of them!)

(qualitatively – the same as for inflation)

1. Fundamental constant Λ
2. Scalar field (with $m \sim 10^{-33}$ eV, $w_{DE} \geq -1$)
3. Geometrical DE = modified gravity (e.g., scalar-tensor and $f(R)$ DE models

Comments about "cosmic coincidences" for Λ

1. Why small? Not known why so small, but all known dimensionless densities are very small

$$\rho_{DE} \sim \rho_{water}^{4/3} \sim m_\nu^4$$

2. Why now? Not an independent problem. Reduces to the first problem (plus relations between other fundamental constants) once "now" is defined in an objective way.

It is natural to use (weak) anthropic principle to define "now". However, in practice, very remote arguments are used.

Example. Let us, following Dicke, define $t_0 \sim t_{\substack{\text{active life} \\ \text{main sequence} \\ \text{star}}} \sim t_{Pl} \cdot \left(\frac{M_{Pl}}{m_p}\right)^3$

Then the "second coincidence problem" is reduced to the first one because of the empirical relation

$$\rho_{DE} \sim \left(\frac{m_p}{M_{Pl}}\right)^6$$

One constant — one problem ("coincidence")

Basic quantities in the reconstruction approach

Order	Geometrical	Physical
1	$H(z) \equiv \frac{\dot{a}}{a}$ $H(0) = H_0$	$\varepsilon_m = \frac{3H_0^2}{8\pi G} \cdot \Omega_{m0}(1+z)^3$ $\varepsilon_{DE} = \frac{3H^2}{8\pi G} - \varepsilon_m$
2	$q(z) \equiv -\frac{\ddot{a}a}{\dot{a}^2}$ $= -1 + \frac{d\ln H}{d\ln(1+z)}$ $q(0) = q_0$ For $\varepsilon_\Lambda = \text{const}$: $q(z) = -1 + \frac{3}{2}\Omega_m(z)$	$V(z)$; $T(z) \equiv \frac{\dot{\varphi}^2}{2}$ $\Omega_V = \frac{8\pi G V}{3H^2}$; $\Omega_T = \frac{8\pi G T}{3H^2}$ $\Omega_V = \frac{2-q}{3} - \frac{H_0^2}{2H^2}\Omega_{m0}(1+z)^3$ $\Omega_T = \frac{1+q}{3} - \frac{H_0^2}{2H^2}\Omega_{m0}(1+z)^3$
3	$r(z) \equiv \frac{\dddot{a}a^2}{\dot{a}^3}$ $r(0) = r_0$ For $\varepsilon_\Lambda \equiv \text{const}$: $r \equiv 1$	$\Pi(z) \equiv \dot{\varphi}V'$ $\Omega_\Pi = \frac{8\pi G \dot{\varphi} V'}{3H^3}$ $\Omega_\Pi = \frac{1}{3}\left(r - 3q - 4 + \frac{9H_0^2}{2H^2}\Omega_{m0}(1+z)^3\right)$

Derivative quantity:

$$w = \frac{T-V}{T+V} = \frac{2q-1}{3\left(1 - \frac{H_0^2}{H^2}\Omega_{m0}(1+z)^3\right)}$$

$w \geq -1$ – "normal" DE

$w < -1$ – "phantom" DE

Λ: $w \equiv -1$

CLASSICAL COSMOLOGICAL TESTS AND THEIR INVERSION

(RECONSTRUCTION OF H(z))

1. High-z supernovae test

$$D_L(z) = a_0(\eta_0 - \eta)(1+z), \qquad \eta = \int_0^t \frac{dt}{a(t)}$$

$$H(z) = \frac{da}{a^2 d\eta} = -(a_0\eta')^{-1} = \left[\left(\frac{D_L(z)}{1+z}\right)'\right]^{-1}$$

2. Angular size test

$$\theta(z) = \frac{d}{a(\eta)(\eta_0 - \eta)} = \frac{d(1+z)}{a_0(\eta_0 - \eta)}$$

$$H(z) = -(a_0\eta')^{-1} = \left[d\left(\frac{1+z}{\theta(z)}\right)'\right]^{-1}$$

3. Volume element test

$$\frac{dN}{dz\,d\Omega} \sim \frac{dV}{dz\,d\Omega} = a^3 r^2 \left|\frac{dr}{dz}\right| =$$

$$= a^3 (r_0 - r)^2 \left|\frac{dr}{dz}\right| = f_V(z)$$

$$f_V(z) = \frac{1}{(1+z)^3 H(z)} \left(\int_0^z \frac{dz}{H(z)} \right)^2$$

$$H^{-1}(z) = \frac{d}{dz} \left\{ \left(3 \int_0^z f_V(z')(1+z')^3 dz' \right)^{1/3} \right\}$$

4. Ages of old objects at high z

$$T(z) > t_i(z)$$

$$T(z) = \int_z^\infty \frac{dz'}{(1+z')H(z')}$$

$$H(z) = -\left((1+z) \frac{dT(z)}{dz} \right)^{-1}$$

5. High-z clustering tests

For $\lambda \ll \lambda_{\gamma,y} \sim R_h$:

$$\ddot{\delta} + 2H\dot{\delta} - \frac{3}{2}\frac{C}{a^3}\delta = 0$$

May be more complicated for geometric dark energy

$$\frac{d}{dt} = aH\frac{d}{da}$$

$$C = \Omega_m H_0^2 a_0^3$$

$$H^2(a) = \frac{3C}{\delta'^2 a^6}\int_0^a \delta\delta' a\,da$$

$$a = \frac{a_0}{1+z}$$

$$\frac{H^2(z)}{H_0^2} = 3\Omega_m \frac{(1+z)^2}{\left(\frac{d\delta}{dz}\right)^2}\int_z^\infty \delta\left|\frac{d\delta}{dz}\right|\frac{dz}{1+z} =$$

$$= \frac{(1+z)^2\delta'^2(0)}{\delta'^2(z)} - \frac{3\Omega_m(1+z)^2}{\delta'^2(z)}\int_0^z \delta\delta'\frac{dz}{1+z}$$

Determination of Ω_m and q_0 from $\delta(z)$:

$$\Omega_m = \frac{\delta'^2(0)}{3\left|\int_0^\infty \delta\delta'\frac{dz}{1+z}\right|}$$

The textbook expression

(Weinberg, Peebles, etc.)

$$\delta(z) \propto H(z) \int_z^\infty \frac{(1+z')\,dz'}{H^3(z')}$$

Theorem

It is valid if and only if

$$H^2(z) = c_1 + c_2(1+z)^2 + c_3(1+z)^3$$

$$\longleftrightarrow$$

The super-Hubble solution ($k \ll aH$)

$$\delta(z) \propto a\left(1 - \frac{H}{a}\int a\,dt\right)$$

Valid for subhorizon scales if

$$H^2(z) = c_1 + c_2(1+z)^3$$

$$\longleftrightarrow$$

From 2dF survey: $\frac{d\ln\delta}{d\ln(1+z)} = -0.51 \pm 0.11$

$z = 0.15$

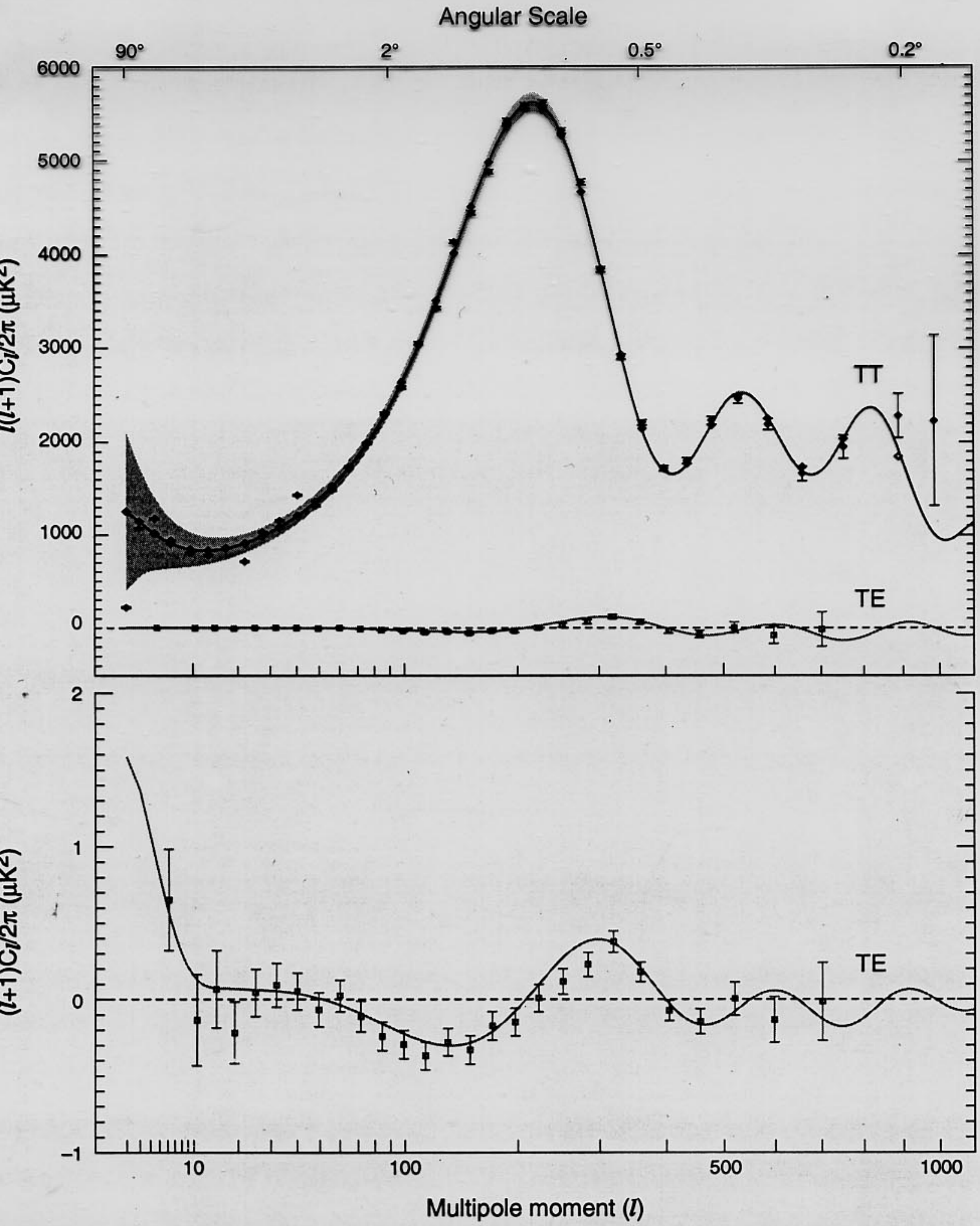

Fig. 22.— Angular power spectra C_l^{TT} & C_l^{TE} from the three-year *WMAP* data. *top*: The TT data are as shown in Figure 16. The TE data are shown in units of $l(l+1)C_l/2\pi$, on the same scale as the TT signal for comparison. *bottom*: The TE data, in units of $(l+1)C_l/2\pi$. This updates Figure 12 of Bennett et al. (2003b).

How to determine $\delta(z)$

a) Evolution of clustering with z

$$r_0(z)$$

b) Evolution of rich cluster abundance with z

$$n(\geq M)(z)$$

c) Weak gravitational lensing of galaxies and CMB

$$\Phi(z)$$

6. CMB tests

a) Spacing between acoustic peaks

$$R \equiv \sqrt{\Omega_{m0}}\, H_0 \int_0^{z_{dec}} \frac{dz}{H(z)} = 1.70 \pm 0.03$$

(Wang & Mukherjee, 200

Precise but degenerate test

b) Correlation between $\frac{\Delta T}{T}$ and LSS (due to the ISW effect)

7. Sakharov oscillations in $P_0(k)$ (BAO

$$\sqrt{\Omega_{m0}} \left(\frac{H_0}{H(z_1)}\right)^{1/3} \left(\frac{1}{z_1} \int_0^{z_1} dz \cdot \frac{H_0}{H(z)}\right)^{2/3} = 0.469 \pm 0.017$$

$z_1 = 0.35$

(Eisenstein et al., 2005)

M. Tegmark et al., ApJ 606, 702 (2004)

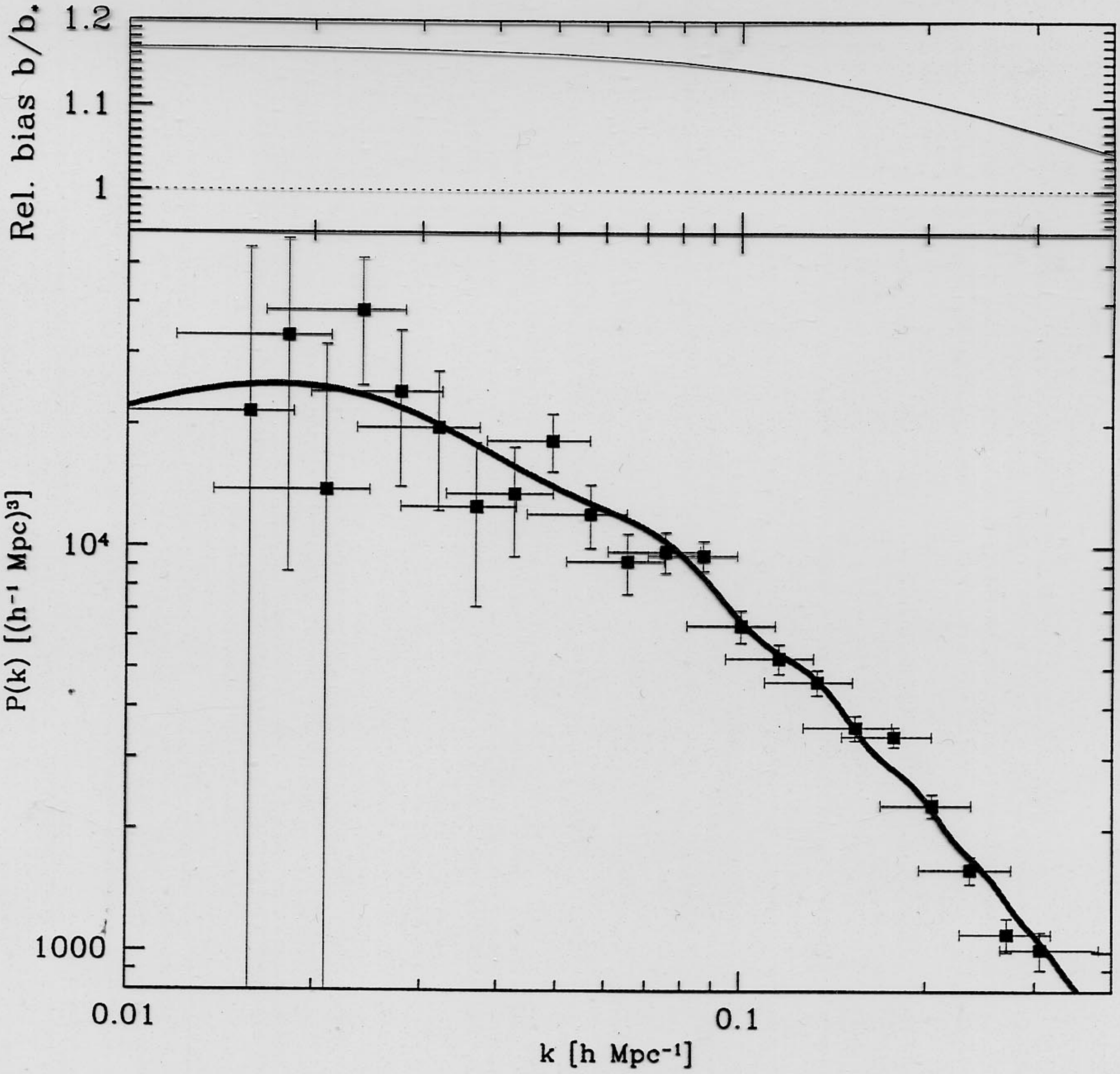

FIG. 22.— The decorrelated real-space galaxy-galaxy power spectrum using the modeling method is shown (bottom panel) for the baseline galaxy sample assuming $\beta = 0.5$ and $r = 1$. As discussed in the text, uncertainty in β and r contribute to an overall calibration uncertainty of order 4% which is not included in these error bars. To remove scale-dependent bias caused by luminosity-dependent clustering, the measurements have been divided by the square of the curve in the top panel, which shows the bias relative to L_* galaxies. This means that the points in the lower panel can be interpreted as the power spectrum of L_* galaxies. The solid curve (bottom) is the best fit linear ΛCDM model of Section 5.

D. E. Eisenstein et al., astro-ph/0501171

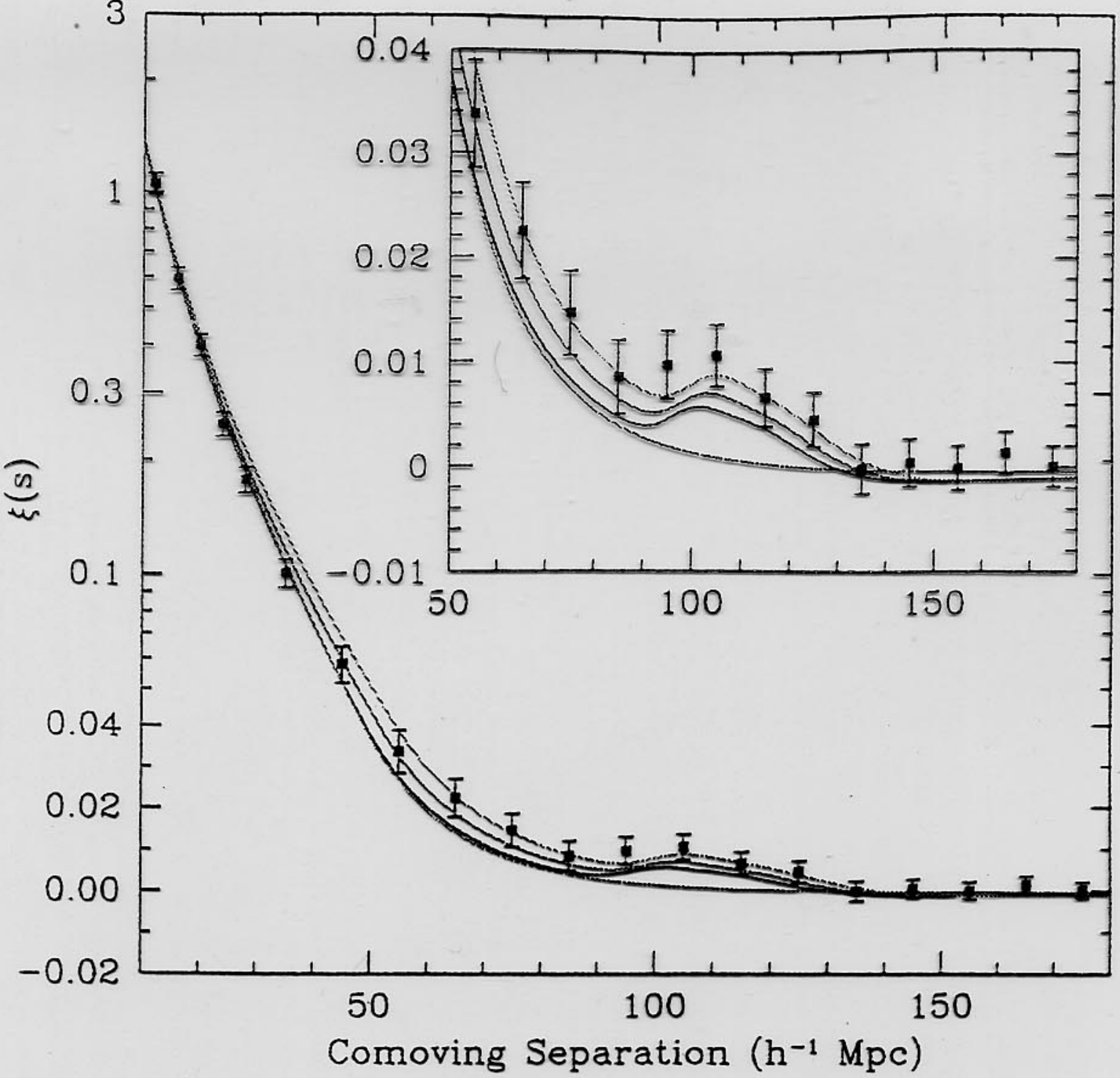

FIG. 2.— The large-scale redshift-space correlation function of the SDSS LRG sample. The error bars are from the diagonal elements of the mock-catalog covariance matrix; however, the points are correlated. Note that the vertical axis mixes logarithmic and linear scalings. The inset shows an expanded view with a linear vertical axis. The models are $\Omega_m h^2 = 0.12$ (top, green), 0.13 (red), and 0.14 (bottom with peak, blue), all with $\Omega_b h^2 = 0.024$ and $n = 0.98$ and with a mild non-linear prescription folded in. The magenta line shows a pure CDM model ($\Omega_m h^2 = 0.105$), which lacks the acoustic peak. It is interesting to note that although the data appears higher than the models, the covariance between the points is soft as regards overall shifts in $\xi(s)$. Subtracting 0.002 from $\xi(s)$ at all scales makes the plot look cosmetically perfect, but changes the best-fit χ^2 by only 1.3. The bump at $100h^{-1}$ Mpc scale, on the other hand, is statistically significant.

$$q_0 = -1 + \left.\frac{d\ln H}{d\ln(1+z)}\right|_{z=0}$$

$\Lambda = \text{const} \longrightarrow H^2(z) = H_0^2\left(1-\Omega_m+\Omega_m(1+z)^3\right)$

$\longrightarrow \quad q_0 = \frac{3}{2}\Omega_m - 1$

II. Reconstruction of $V(\varphi)$ from $H(a)$

$$\begin{cases} 8\pi G V = aH\dfrac{dH}{da} + 3H^2 - \dfrac{3}{2}\Omega_m H_0^2\cdot\left(\dfrac{a_0}{a}\right)^3 \\ 4\pi G\, a^2H^2\left(\dfrac{d\varphi}{da}\right)^2 = -aH\dfrac{dH}{da} - \dfrac{3}{2}\Omega_m H_0^2\left(\dfrac{a_0}{a}\right)^3 \end{cases}$$

Necessary condition $(\varepsilon_{DE} + p_{DE} \geq 0)$

$w_{DE} \equiv \frac{p_{DE}}{\varepsilon_{DE}} \geq -1$

$$\frac{dH^2}{dz} \geq 3\Omega_m H_0^2(1+z)^2$$

$$H^2 \geq H_0^2\left(1+\Omega_m(1+z)^3 - \Omega_m\right)$$

In particular: $\quad q_0 \geq \frac{3}{2}\Omega_m - 1$

No such a condition in case of scalar-tensor gravity

$$\begin{tikzcd}
\mathcal{D}_L(z) \arrow[dr] & & \\
& H(z) \arrow[r, "\Omega_m"] & V(\varphi) \\
\left(\frac{\delta\rho}{\rho}\right)_{CDM}(z) \arrow[ur, "H_0"'] & &
\end{tikzcd}$$

Example of the reconstruction

Let $\Lambda \propto a^{-q}$ or $p_\Lambda = \left(-1+\frac{q}{3}\right)\varepsilon_\Lambda$

$q = \mathrm{const} < 3$

$$H^2(z) = \Omega_m H_0^2 (1+z)^3 + (1-\Omega_m) H_0^2 (1+z)^q$$

$$w = \frac{q-3}{3} < 0$$

$$\frac{a}{a_0} = \left(\frac{\Omega_m}{1-\Omega_m}\right)^{\frac{1}{3-q}} \sinh^{\frac{2}{3-q}}\left((3-q)\sqrt{\frac{2\pi G}{q}}\,(\varphi-\varphi_0+\varphi_1)\right)$$

$$V(\varphi) = \frac{3-\frac{q}{2}}{8\pi G}\cdot\frac{(1-\Omega_m)^{\frac{3}{3-q}}}{\Omega_m^{\frac{q}{3-q}}}\,H_0^2 \times$$

$$\times \frac{1}{\sinh^{\frac{2q}{3-q}}\left((3-q)\sqrt{\frac{2\pi G}{q}}\,(\varphi-\varphi_0+\varphi_1)\right)}$$

$$\varphi_1 = \varphi_1(\Omega_{m0}, q) = \frac{1}{3-q}\sqrt{\frac{q}{2\pi G}}\,\ln\frac{1+\sqrt{1-\Omega_m}}{\sqrt{\Omega_m}}$$

Another interesting example:

$$\varepsilon_\Lambda = \varepsilon_v + \varepsilon_1 \left(\frac{a_0}{a}\right)^3$$

$$H^2 = H_0^2 \left(1 - \Omega_m - \Omega_1 + (\Omega_m + \Omega_1)\left(\frac{a_0}{a}\right)^3\right)$$

$$\varepsilon_v = \frac{3H_0^2}{8\pi G}\left(1 - \Omega_m - \Omega_1\right)$$

$$\varepsilon_1 = \frac{3H_0^2}{8\pi G}\,\Omega_1$$

$$V(\varphi) = \frac{3H_0^2}{8\pi G}\left(1 - \Omega_m - \Omega_1 + A\sinh^2\left(B(\varphi - \varphi_0 + \varphi_1)\right)\right)$$

$$A = \frac{1}{2}\,\frac{\Omega_1(1 - \Omega_m - \Omega_1)}{\Omega_m + \Omega_1}\,; \quad B = \sqrt{\frac{6\pi G(\Omega_m + \Omega_1)}{\Omega_1}}\,;$$

$$\varphi_1 = \sqrt{\frac{\Omega_1}{(\Omega_m + \Omega_1)\,24\pi G}}\,\ln\frac{1 + \sqrt{\Omega_m + \Omega_1}}{1 - \sqrt{\Omega_m + \Omega_1}}$$

$t \to \infty$: $a \to \infty$, $\varphi \to \varphi_0 - \varphi_1$

De Sitter with $m_\Lambda = \frac{3}{2} H_\infty$

$$\boxed{\Omega_1 \lesssim 0.05\,\Omega_m}$$

Reconstruction of $\delta(z)$ from $\mathcal{D}(z)$

$G_{eff}(z) = const$ assumed

Test if DE is physical or geometrical

$$E(z) = H_0 \, \mathcal{D}_L(z)/(1+z) \Rightarrow z(E)$$

$$\delta(E(z)) = \delta(0) + \delta'(0) \int_0^E (1+z(E))\, dE$$
$$+ \frac{3}{2} \Omega_m \int_0^E (1+z(E_1))\, dE_1 \int_0^{E_1} \delta(E_2)\, dE_2$$

Given $\delta'(0)/\delta(0)$, $\delta(z)/\delta(0)$ can be found iteratively

No differentiation of data!

V. Sahni, A.S., IJMPD 15, 2105 (2006)
(astro-ph/0610026)

Practical reconstruction of $H(z)$, $w(z)$, etc. from $D_L(z)$

Explicit or implicit smoothing over some interval Δz is required!

1. Top-hat smoothing
2. Gaussian smoothing MNRAS 366, 1081 (2006)
   (A. Shafieloo et al., astro-ph/0505329)
3. The principal components method
4. Parametric fits (implicit smoothing!)

a).
$$\frac{H^2(z)}{H_0^2} = A_0 + A_1(1+z) + A_2(1+z)^2 + \Omega_m(1+z)^3$$

$$A_0 + A_1 + A_2 + \Omega_m = 1$$

This fit does not exclude a possibility $\varepsilon_{DE} < 0$!

U. Alam et al. MNRAS 354, 275 (2004) [astro-ph/0311364]

U. Alam et al. JCAP 0604, 008 (2004) [astro-ph/0403687]

U. Alam et al. JCAP 0702, 011 (2007) [astro-ph/0612381]

b) The CPL fit

(Chevallier-Polarski-Linder)

$$w(z) = w_0 + w_1\frac{z}{1+z}$$

A. Riess et al., astro-ph/0402512

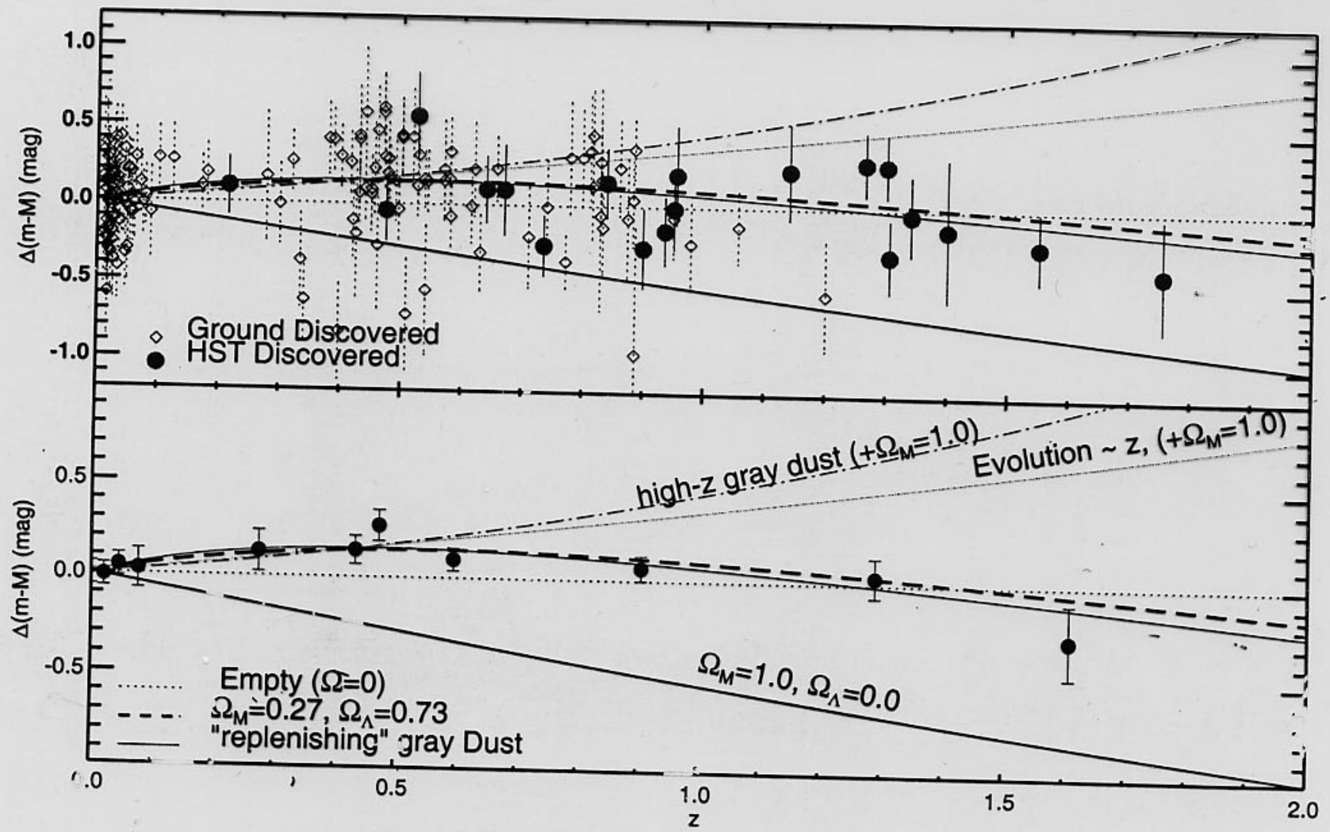

Recent enlargement of the "Gold" sample:

A. Riess et al., astro-ph/0611572

New SNe samples: SNLS

ESSENCE

PRESENT STAGE OF DARK ENERGY RECONSTRUCTION

1. In the first approximation, DE is well described by a cosmological constant

$$w_{DE} \simeq -1$$

2. $w_{DE} = -1$ is inside 2σ error bars for all data

3. If $w_{DE} = const \neq -1$, then

$$|w_{DE} + 1| \lesssim 0.1$$

E.g. W.J. Percival et al., arXiv: 0705.3323

$$w_{DE} = -1.004 \pm 0.089$$

4. No evidence for permanent phantom DE.
No evidence for the Big Rip in future

$(\Delta T > 50 \text{ byl. y.})$ $\quad a(t) \propto (t_1 - t)^{-p}$, $p > 0$

However

5. SNe: small discrepancy between Gold and SNLS samples

BAO: comparison of $D_V(0.2)$ with $D_V(0.35)$ slightly favors $w_{DE} < -1$ for $z < 0.35$

6. If the assumption $w_{DE} = \mathrm{const}$ is omitted, some place for 'temporary phantom' DE still exists for $z \lesssim 0.3$

But $\overline{w}_{DE}\,(0 < z \lesssim 0.4) \simeq -1$

7. Place for dynamical dark energy (especially, a geometric one) still exists!

Recent review on the reconstruction approach:

V. Sahni, A.A. Starobinsky, IJMPD 15, 2105 (2006) [astro-ph/0610026

U. Alam, V. Sahni, A. S., astro-ph/0612381
JCAP 0702, 011 (2007)

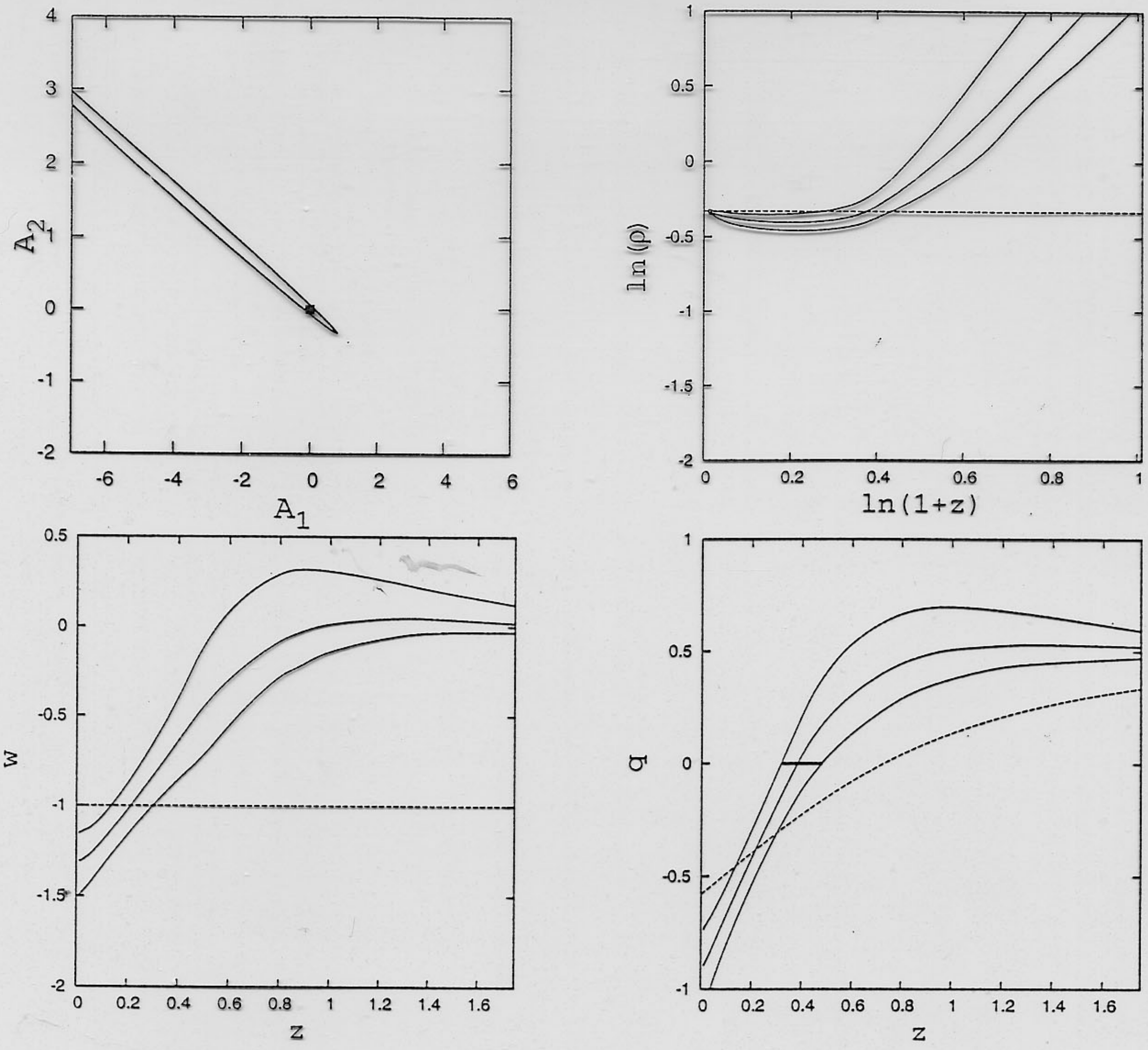

FIG. 2: 2σ confidence levels for the Gold dataset using $\Omega_{0m} = 0.28 \pm 0.03$. The upper left hand panel shows the confidence levels in $A_1 - A_2$, with the black dot representing ΛCDM. The upper right hand panel shows the logarithmic 2σ variation of the DE density in terms of redshift. The dashed line represents ΛCDM. The lower left and right hand panels represent the variation of the equation of state and deceleration parameter respectively. The dashed lines in both panels represent ΛCDM. The thick solid line in the lower right hand panel shows the acceleration epoch, i.e. the redshift at which the universe started accelerating.

$$\frac{H^2(z)}{H_0^2} = A_0 + A_1(1+z) + A_2(1+z)^2 + \Omega_m(1+z)^3$$

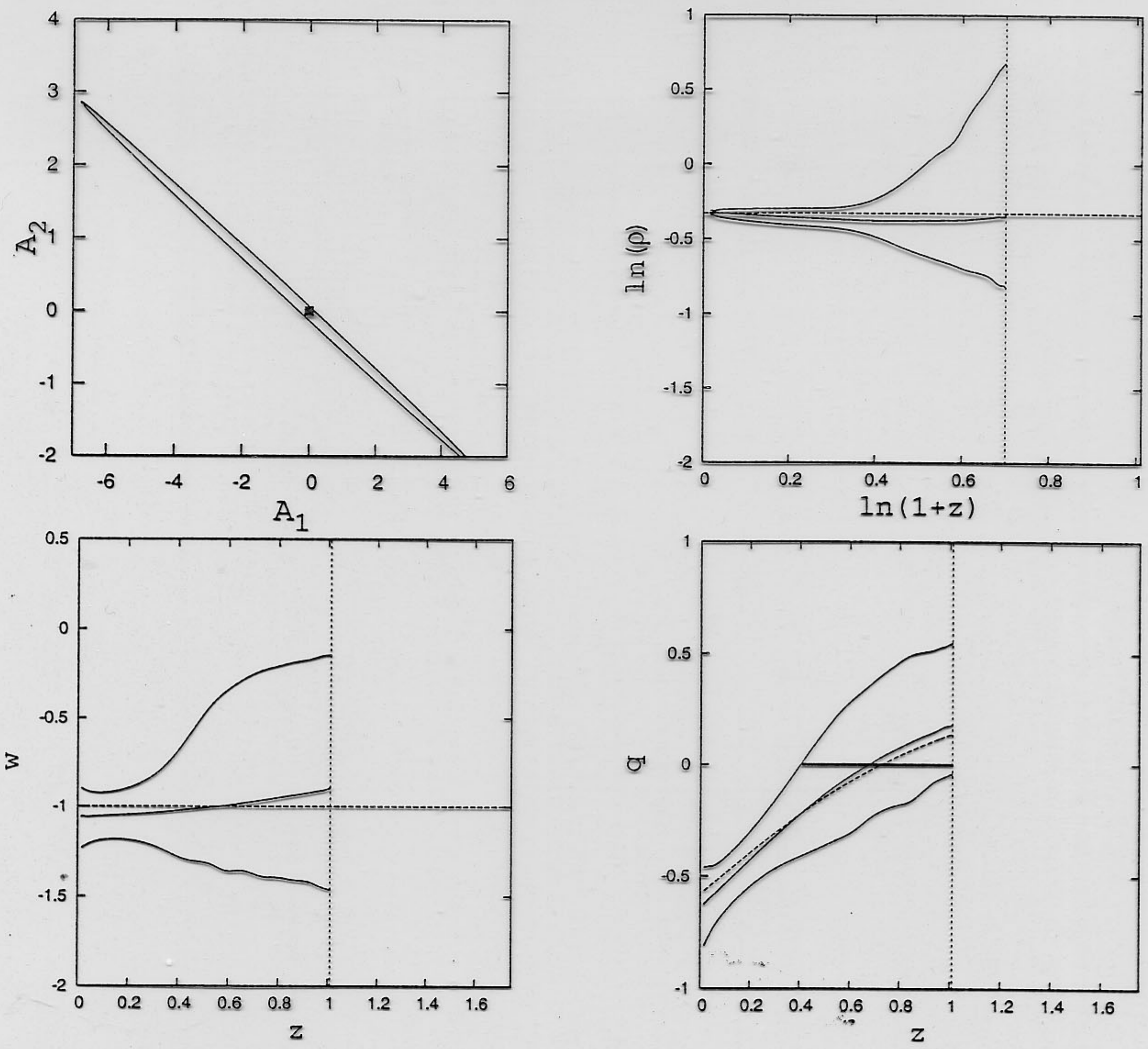

FIG. 3: 2σ confidence levels for the SNLS dataset using $\Omega_{0m} = 0.28 \pm 0.03$. The upper left hand panel shows the confidence levels in $A_1 - A_2$, with the black dot representing ΛCDM. The upper right hand panel shows the logarithmic 2σ variation of the DE density in terms of redshift. The dashed line represents ΛCDM. The lower left and right hand panels represent the variation of the equation of state and deceleration parameter respectively. The dashed lines in both panels represent ΛCDM. The thick solid line in the lower right hand panel shows the acceleration epoch, i.e. the redshift at which the universe started accelerating. Results are shown upto $z = 1.01$

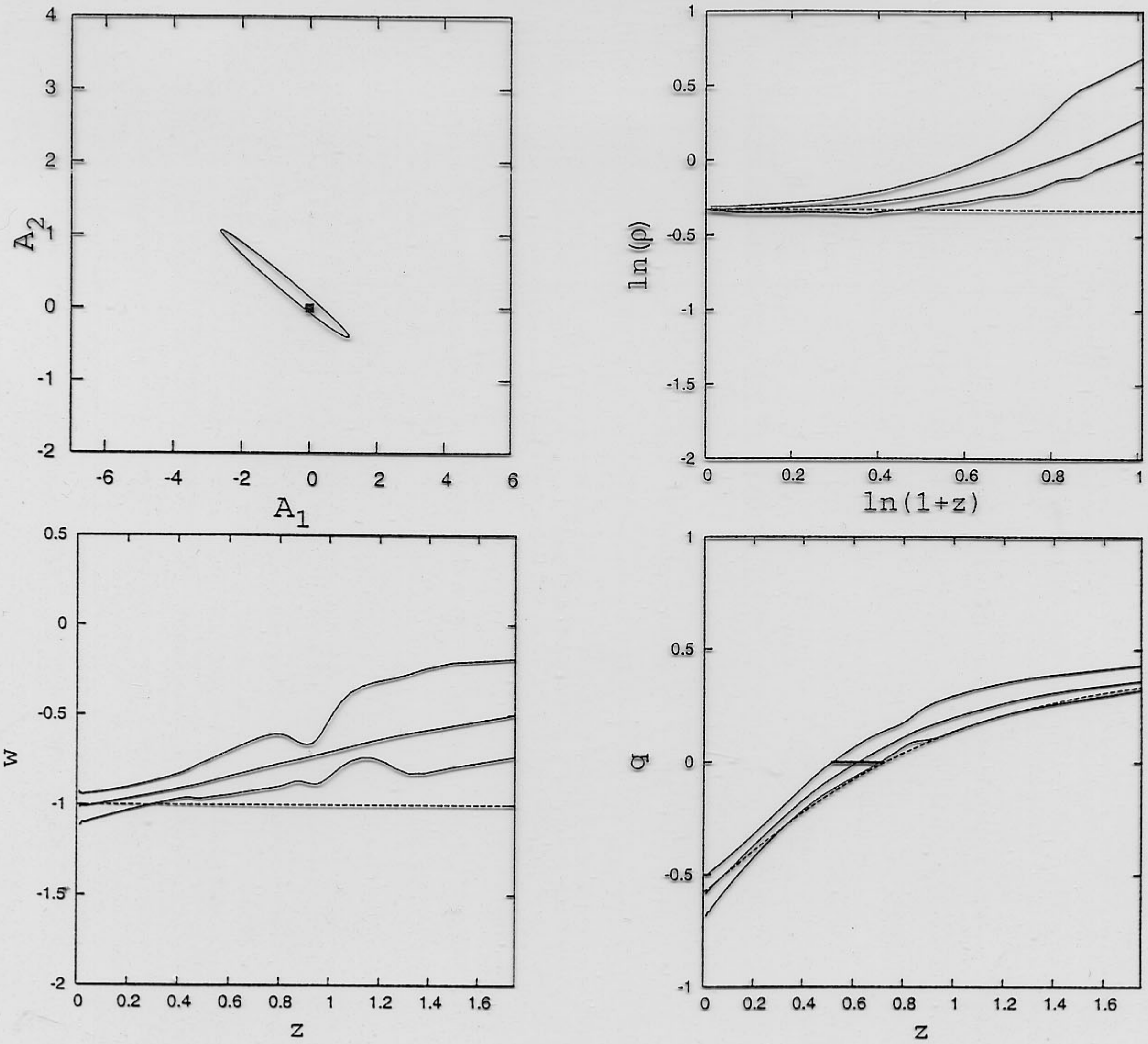

FIG. 6: 2σ confidence levels for the Gold+CMB+BAO dataset using $\Omega_{0m} = 0.28 \pm 0.03$. The upper left hand panel shows the confidence levels in $A_1 - A_2$, with the black dot representing ΛCDM. The upper right hand panel shows the logarithmic 2σ variation of the DE density in terms of redshift. The dashed line represents ΛCDM. The lower left and right hand panels represent the variation of the equation of state and deceleration parameter respectively. The dashed lines in both panels represent ΛCDM. The thick solid line in the lower right hand panel shows the acceleration epoch, i.e. the redshift at which the universe started accelerating.

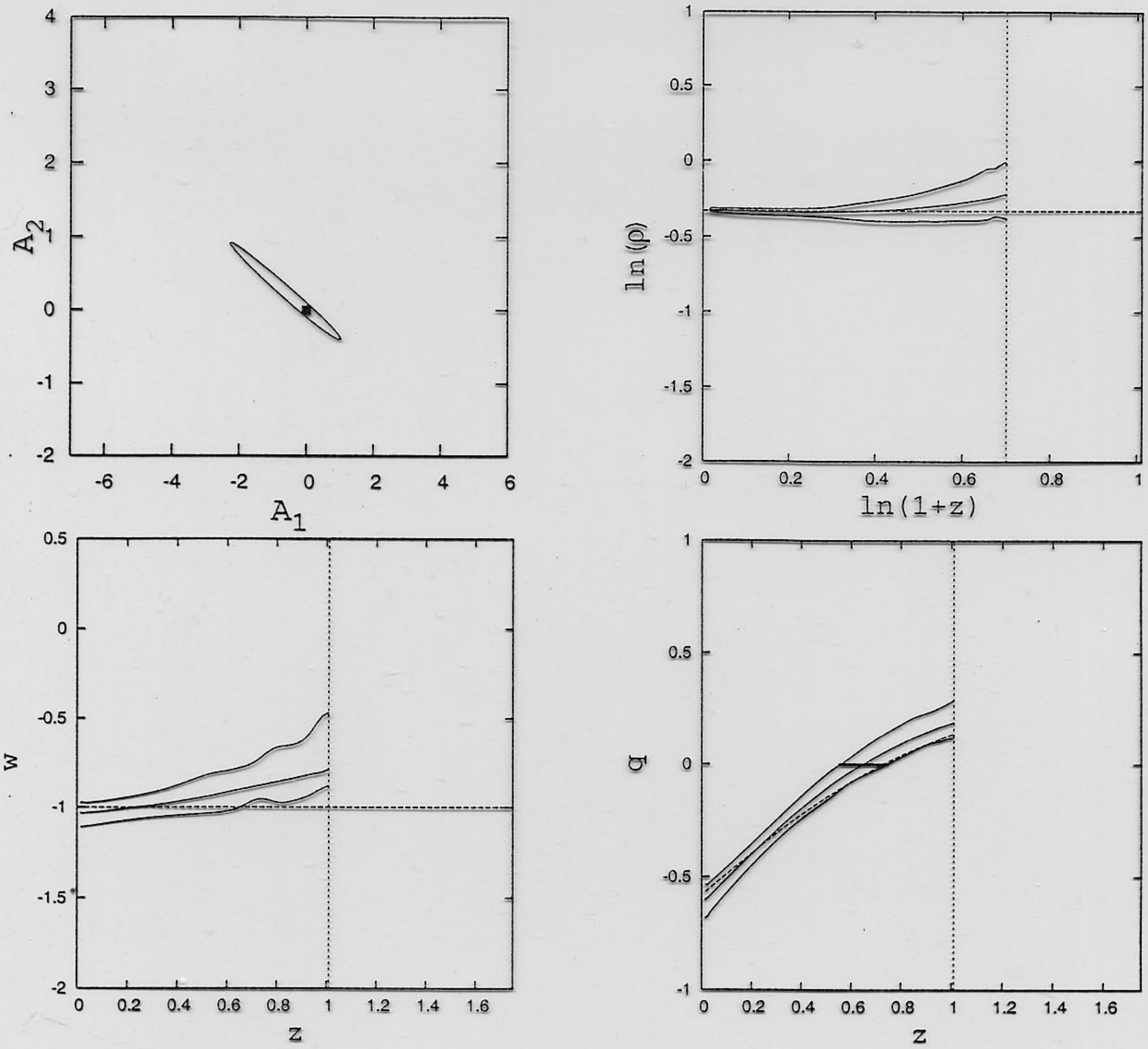

FIG. 7: 2σ confidence levels for the SNLS+CMB+BAO dataset using $\Omega_{0m} = 0.28 \pm 0.03$. The upper left hand panel shows the confidence levels in $A_1 - A_2$, with the black dot representing ΛCDM. The upper right hand panel shows the logarithmic 2σ variation of the DE density in terms of redshift. The dashed line represents ΛCDM. The lower left and right hand panels represent the variation of the equation of state and deceleration parameter respectively. The dashed lines in both panels represent ΛCDM. The thick solid line in the lower right hand panel shows the acceleration epoch, i.e. the redshift at which the universe started accelerating. Results are shown upto redshift $z = 1.01$